Journal of Power Sources 426 (2019) 47–54

Contents lists available at ScienceDirect

Journal of Power Sources

journal homepage: www.elsevier.com/locate/jpowsour

Biopolymer-based carboxylated chitosan hydrogel film crosslinked by HCl as gel polymer electrolyte for all-solid-sate supercapacitors

Hezhen Yang[b], Ying Liu[a,b], Lingbin Kong[a,b], Long Kang[a,b], Fen Ran[a,b,*]

[a] State Key Laboratory of Advanced Processing and Recycling of Non-ferrous Metals, Lanzhou University of Technology, Lanzhou, 730050, PR China
[b] School of Material Science and Engineering, Lanzhou University of Technology, Lanzhou, 730050, Gansu, PR China

HIGHLIGHTS

- Gel polymer electrolyte of carboxylated chitosan hydrogel is prepared by phase-separation.
- HCl is the key chemical for crosslinking for forming transparent and flexible film.
- Exhibiting electrolyte uptake rate of 742.0 wt% and ionic conductivity of 8.69×10^{-2} S cm^{-1}.
- Capacitance of 45.9 F g^{-1}, energy density of 5.2 Wh kg^{-1}, and power density of 226.6 W kg^{-1}.

ARTICLE INFO

Keywords:
Chitosan
Film
Gel polymer electrolyte
Ionic conductivity
All-solid-sate
Supercapacitors

ABSTRACT

Gel polymer electrolyte for flexible energy storage devices such as supercapacitors and rechargeable batteries attracts widespread attentions. Herein, we fabricate a flexible, transparent, and eco-friendly gel polymer electrolyte film based on biodegradable polymer of the carboxylated chitosan via phase separation of carboxylated chitosan hydrogel in hydrochloric acid. HCl is the key chemical for crosslinking of film forming, and the process is simple, rapid and non-polluting. The obtained carboxylated chitosan hydrogel film with excellent flexibility exhibits a highest electrolyte uptake rate of 742.0 *wt*%, and a highest ionic conductivity of 8.69×10^{-2} S cm^{-1}. A symmetric all-solid-state supercapacitors using carbon cloth as current collectors, activated carbon film as electrodes, and carboxylated chitosan hydrogel film as a gel polymer electrolyte shows a high specific capacitance of 45.9 F g^{-1} at 0.5 A g^{-1}, and the maximum energy density of 5.2 Wh kg^{-1} at a power density of 226.6 W kg^{-1}. To our knowledge, this is the first time that carboxylated chitosan hydrogel film being used as gel polymer electrolyte for supercapacitors electrolyte. The good results indicate that the carboxylated chitosan as a new gel polymer electrolyte material has great potential in practical applications of all-solid-state, flexible, and portable energy storage devices.

1. Introduction

In recent years, with the prospering development of portable, flexible, and wearable electronic devices, flexible energy storage devices have become a research hotspot [1–4]. Among them, it is well known that supercapacitors have many advantages such as rapid charging/discharging ability, long cycle life, superior power density, and good eco-friendliness [5]. In general, the performance of supercapacitors depends on electrode, electrolyte and device configuration [6,7]. There have been many works concerning electrode materials, while these focusing on the electrolytes of supercapacitors are rather limited [8,9]. However, electrolyte is one of the key components, which determines electrochemical stable potential window, cycle life, and safety of supercapacitors [10,11]. In particular, gel polymer electrolytes (GPEs) for supercapacitors have been developed, for example, a chemically crosslinked PVA-H_2SO_4 hydrogel film synthesized by adding glutaraldehyde that acted as a crosslinking reagent, which showed excellent elasticity, high mechanical strength, and ionic conductivity after being constructed as an integrated flexible supercapacitor [12]. When a zwitterionic gel electrolyte of poly(propylsulfonate dimethylammonium propylmethacrylamide) applied to graphene-based solid-state supercapacitor, it obtained superior electrochemical performance [13]. Vinyl hybrid silica nanoparticle comprising polyacrylamide backbones dual cross-linked hydrogel was presented. As a result, supercapacitor

* Corresponding author. State Key Laboratory of Advanced Processing and Recycling of Non-ferrous Metals, Lanzhou University of Technology, Lanzhou, 730050, PR China.
E-mail addresses: ranfen@163.com, ranfen@lut.cn (F. Ran).

https://doi.org/10.1016/j.jpowsour.2019.04.023
Received 1 March 2019; Received in revised form 2 April 2019; Accepted 6 April 2019
Available online 12 April 2019
0378-7753/

with this electrolyte can be stretched up to the unprecedented 1000% strain with enhanced performance, and compressed to 50% strain with initial performance [14]. Although these GPEs have been applied to supercapacitors with good performance, the preparation processes are pretty complex. What's more, all these conventional polymer matrix materials are generally not biodegradable. The environmental pollution caused by these synthetic polymers, which are difficult to be decomposed, has brought about serious problems. It makes sense to use inherent degradable biopolymers instead of non-degradable synthetic polymers. For example, the chitosan-based hydrogels have been reported as electrolyte materials for supercapacitors [15,16]. Whereas, pure chitosan film has very low ionic conductivity, and very low proton conductivity ($\sim 10^{-9}$ S cm^{-1}) in dry chitosan film without any structural modification [17,18]. So several methods such as combining with lithium and ammonium salts, adding plasticizers, and blending with different polymers have been used to enhance its ionic conductivity [19–23]. Furthermore, chitosan generally dissolves in dilute acid solution, which seems to limit its wider applicability due to its poor solubility in water [24]. Carboxylated chitosan is a derivative of chitosan, which has many advantages and widely been used. Not only does it has biocompatibility, biodegradability, nontoxicity, antimicrobial activity, strong affinity, and film-forming property like chitosan, but also it is a water-soluble derivative rich in amino group, hydroxyl group, and carboxyl group increasing the absorption of solution [25–28]. Importantly, carboxylated chitosan is an amphoteric polyelectrolyte with pH sensitivity [29,30]. It is commonly applied in drug delivery, tissue engineering, cosmetics, and food industry [31–33]. However, the studies involving usage of carboxylated chitosan as electrolyte material to supercapacitors have not been reported.

Here, a flexible GPE film with high conductivity based on green biopolymer-carboxylated chitosan was developed via the solution coating and crosslinking by hydrochloric acid. The film preparation process was simple, quick, and environmentally friendly compared to the multi-step synthesis and purification process [34,35]. All-solid-state electronic double layer capacitor (EDLC) was assembled with carboxylated chitosan film as the polymer electrolyte, activated carbon film as the electrodes, and carbon cloth as collectors. The device showed an outstanding electrochemical performance with high specific capacitance and energy density. It is believed that GPE based on carboxylated chitosan would have a broad prospect in the applications in energy storage devices.

2. Experimental

2.1. Chemicals

Carboxylated chitosan was purchased from *Aladdin*. Polyether sulfone (PES, Ultrason E6020P) was obtained from *BASF*, Germany. Activated carbon was provided by *Shenyang Kejing Auto-instrument Co. Ltd*. Carbon cloth was bought from *Hubei rocktech instrument Co. Ltd, China*. All other chemical reagents such as hydrochloric acid (HCl) and dimethylacetamide (DMAC) were obtained from *Sinopharm Chemical Reagents Co. Ltd*, *China*, and used without further purification.

2.2. Preparation of CCH film

1.0 g of carboxylated chitosan power was dissolved in 10 ml deionized water at room temperature under magnetic stirring to form carboxylated chitosan casting solution. Afterwards, it made the casting solution stand for a while to remove air bubbles and then coat casting to the glass plate. The casting solution was prepared as film by spin coating and the film thickness was controlled by spin coating (Spin Coater, KW-4A) at a rotating speed of 500 rpm/min for 6 s. Finally, the glass plate with casting solution was subjected to crosslinking through immersion in hydrochloric acid solution for 6 h. The thickness of CCH film was 0.532 mm.

2.3. Determination of isoelectric point of carboxylated chitosan

Turbidity experiments were used to determine IEP (isoelectric point) of carboxylated chitosan. The carboxylated chitosan solution with a concentration of 0.1 g/ml was configured. Aqueous solutions with various pHs was prepared by 0.01 mol/l HCl and 0.01 mol/l NaOH, respectively. PerkinElmer Lambda 25 UV–visible spectrometer was used to determine the transmittance of the carboxylated chitosan solution in aqueous solutions with various pHs, and then IEP was obtained.

2.4. Characterizations of CCH film

The morphologies of sample were observed by field emission scanning electron microscope (SEM, JSM-6701F, JEOL, Japan). The crystal structure was analyzed by X-ray diffraction (XRD Bruker, D8 Advance, Germany). Fourier transform infrared spectroscopy (FTIR) spectra of KBr tablet were measured with FTIR Nexus 670 instrument. The thermal stability of the prepared film was determined using thermogravimetric analysis (TGA/DSC, Mettler Toledo) under nitrogen atmosphere from room temperature to 800 °C at 10 °C/min heating rate. The sample of CCH film for these characterizations dealt with freeze-drying method.

The ionic conductivity of the film was calculated by the equation of $\sigma = L/(R_b A)$, where L was the thickness (cm) of the CCH film, A was the effective contact area (cm^2) of the film with the steel electrodes, and R_b was the bulk resistance (Ω) obtained from the first intercept on the x-axis of the impedance figure [36]. R_b was measured by sandwiching the CCH film with two stainless steel sheets of 1.3 × 1.3 cm^2 on a CHI660E electrochemical workstation. The electrolyte uptake rate of the film (W) was estimated using the following equation: $W\% = M_{wet} - M_{dry}/M_{dry} \times 100\%$, where M_{dry} was the dry weight of film after being dried in an oven at 50 °C, and M_{wet} was the wet weight of film after soaking in HCl electrolyte at room temperature for 6 h.

2.5. Electrode preparation

The flexible film electrode was fabricated based on the liquid-liquid phase-separation technique of polyethersulfone according to our previous report [37]. For the preparation of activated carbon (AC) film electrode, a thin film of about 1.2 × 1.2 cm^2 was cut from the membrane. The capacitance value was calculated based on the electro-active material used in the film.

2.6. Assembly of all-solid-state EDLC

All-solid-state EDLC was assembled with the CCH film, symmetric activated carbon film electrodes, and carbon cloths (used as the current collectors). The CCH film was sandwiched between two activated carbon films and pressed carbon cloths on them together under a pressure.

2.7. Electrochemical performance

The electrochemical performance of the all-solid-state EDLC was examined by cyclic voltammetry (CV) measurement, galvonostatic charging-discharging (GCD) measurement, and electrochemical impedance spectroscopy (EIS) test on a CHI660E (Shanghai, China) electrochemical workstation in a two-electrode mode. The cycle stability test was measured on a land cell tester.

For the all-solid-state EDLC, the specific capacitance of device were calculated by the following equation (1):

$$C = I \times t/(\triangle V \times m) \quad (1)$$

where C (F g^{-1}) was the specific capacitance, I (A) was discharging

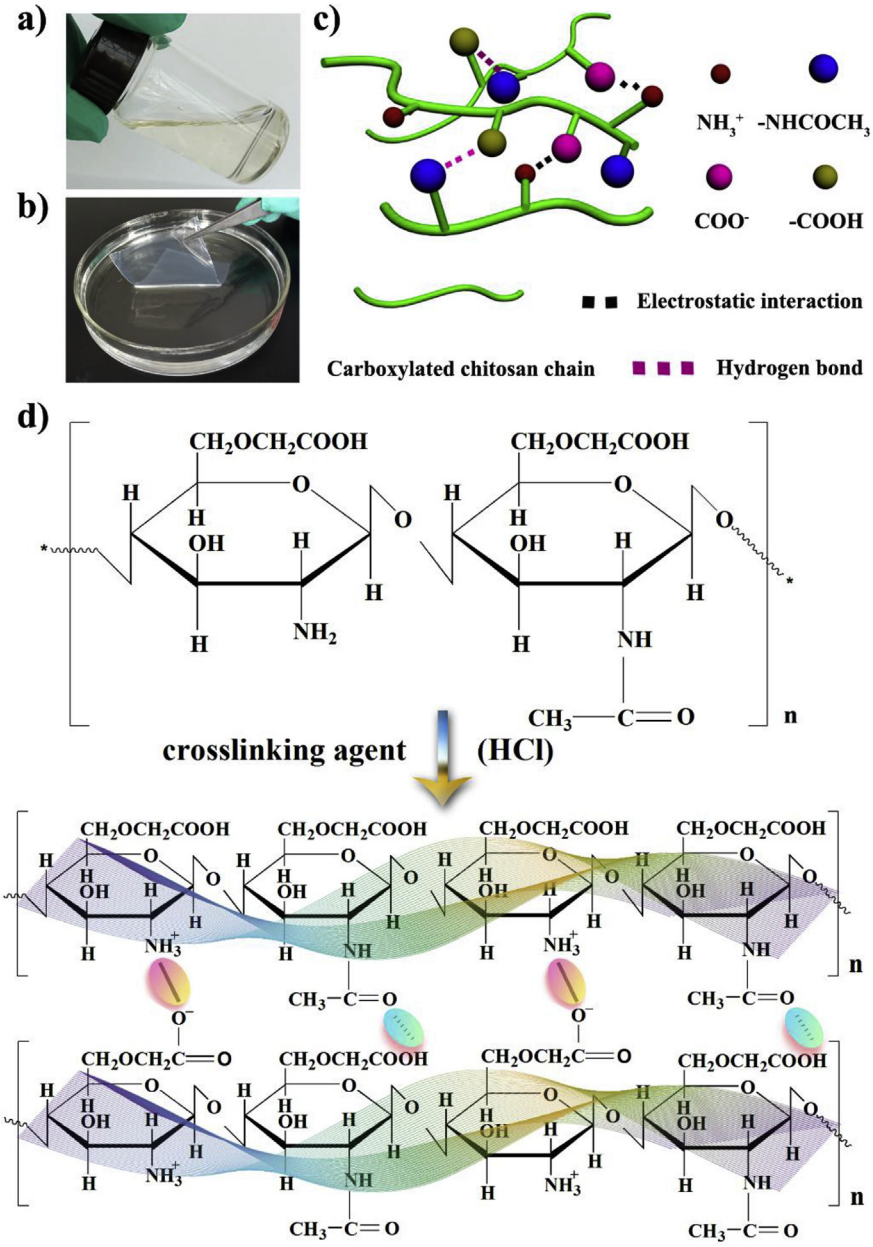

Fig. 1. a) Digital photos of carboxylated chitosan solution, b) crosslinked CCH film, and (c and d) schematic illustration of internal crosslinking for CCH film.

current, t (s) was the discharging time, $\triangle V$ (V) was the potential drop during discharging process, and m (g) was the mass of active materials.

The energy and power density of device were calculated from the discharging curves at different current densities according to equations (2) and (3):

$$E = C \times V^2/(2 \times 3.6) \quad (2)$$

$$P = E \times 3600/(\triangle t) \quad (3)$$

where E (Wh kg^{-1}) was the energy density of device, C (F g^{-1}) was the specific capacitance, V (V) was the potential drop during discharging process, P (W kg^{-1}) was the power density of device, and $\triangle t$ (s) was the discharging time, respectively.

3. Results and discussion

Gel polymer electrolyte (GPE) film was prepared based on the biodegradable polymer of the carboxylated chitosan via phase separation method of CCH in hydrochloric acid (HCl). In a nutshell, commercial carboxylated chitosan power was dissolved in deionized water at room temperature under magnetic stirring to form carboxylated chitosan casting solution (see Fig. 1a). One can see that the casting solution formed of 1 g carboxylated chitosan dissolved in 10 ml distilled water was transparent, uniform, and flowing. The glass plate with casting solution was subjected to crosslinking through immersion of it in hydrochloric acid solution for 6 h. During this process, when the crosslinking happened and the casting solution transferred into CCH film, it cannot dissolve in 1 mol/l hydrochloric acid solution as shown in Fig. 1b. It should be noted that the crosslinking process and the film preparation process was very rapid within two minutes.

For the film fabrication, HCl was the key chemical crosslinking agent, and we vividly described the internal crosslinking mechanism as shown in Fig. 1c. In fact, the polymer chains were perfectly crosslinked forming an interconnected bulk through both electrostatic attraction and hydrogen bonds interaction. The macromolecular structure evolution and the functional groups forming for crosslinking are further

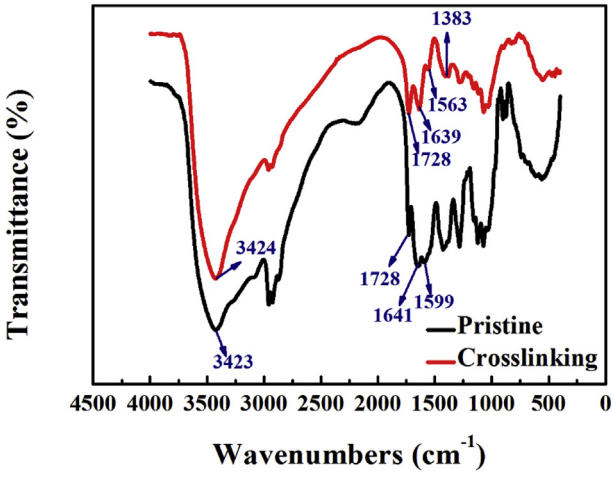

Fig. 2. FTIR spectra of pristine carboxylated chitosan powders and CCH film.

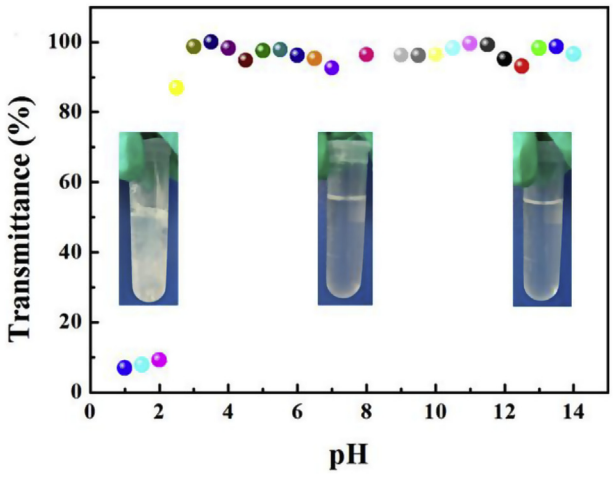

Fig. 3. IEP determination of carboxylated chitosan solution by turbidity measurement.

illustrated in Fig. 1d. As one can see that the carboxylated chitosan polymer chains would possess high electrolyte absorption ability due to the large number of hydrophilic groups such as -NH_2, -OH, -COOH, and -NHCO-. Interestingly, under the circumstance of HCl solution, -NH_2 on carboxylated chitosan chains was protonized into -NH_3^+ [38]. In this case, a large number of -COOH and a small number of COO^- existed in acidic condition, and two kind of non-covalent bonds formed including the ionic bond between NH_3^+ and COO^-, and hydrogen bond between -COOH and -$NHCOCH_3$. Finally, carboxylated chitosan chains were cross-linked and achieved high film properties.

Pristine carboxylated chitosan powder (CCP) and the crosslinking CCH were characterized by FTIR as shown in Fig. 2. For CCP, the strong characteristic absorption of the peak between 3300 cm^{-1} and 3500 cm^{-1} was observed in the spectrum, which was attributed to the stretching vibration of *N*-H (primary amine) and *O*-H groups displayed strong hydrogen bond interactions [39]. After being crosslinked by HCl, this band became narrow and shifted to the higher wavenumber region, ascribing to the protonation of NH_2 group, which changed original hydrogen bond structure. Meanwhile, in the spectrum of pristine CCP, there were two peaks appeared at 1728 cm^{-1}, belonging to the C=O stretching vibration in -COOH, and one at 1641 cm^{-1} corresponding to the C=O stretching vibration in -$NHCOCH_3$. The deformation vibration of *N*-H in -NH_2 appeared at 1599 cm^{-1}. After crosslinking, the appearance of two new peaks at 1563 cm^{-1} and 1383 cm^{-1} were assigned to the deformation vibration of NH_3^+ and C=O stretching vibration in $-COO^-$, respectively. It illustrated the existence of ion interaction between the positively charged NH_3^+ and negatively charged $-COO^-$ in carboxylated chitosan chain. In addition, the absorption peak at 1641 cm^{-1} shifted to 1639 cm^{-1}, which revealed hydrogen bonding between -$NHCOCH_3$ and -COOH.

Isoelectric point (IEP) is one of the important parameters for estimating the application of amphoteric polyelectrolytes. Under certain pH condition, if the average charge on the chain of amphoteric polyelectrolyte macromolecule were zero, this pH value would be the IEP (isoelectric point) of this amphoteric polyelectrolyte. In the range of IEP, groups with opposite charges attracted to each other, resulting in decrease of the solubility of molecular chains in the solution [40]. The IEP of carboxylated chitosan solution was determined by turbidity measurements [41,42], and the results are shown in Fig. 3. As can be seen from the diagram, the range of IEP for carboxylated chitosan was less than 2. It is proved that the carboxylated chitosan solution would be insoluble in a solution with any pH values less than 2. So the illustration shows that the carboxylated chitosan solution forming gel would lead to reduction of transmittance; while when external solution with a pH value higher than 2, carboxylated chitosan could dissolve in the solution. Based on the experiments, one can see that both solutions of carboxylated chitosan at the values of 6 and 12 were transparent, while that at the value of 1 was murky. These results further explain that the state of carboxylated chitosan solution could be used to realize the crosslinking of the polymer macromolecules in strong acidic solution.

The formation of crosslinking bonds among carboxylated chitosan chains through HCl was confirmed by indissolubility of film immersed in water for different time, and XRD and TGA-DSC characterizations as shown in Fig. 4 As can be seen from Fig. 4a, CCH film remained intact and did not dissolve after being soaked in water for even one week. These results exhibited that the prepared film had good stability in water. The CCH film before being freeze-dried could be bent for any angles (see Fig. 4b). After freeze-drying, the film with thickness of 33 μm was completely transparent as presented in Fig. 4c. It is important that the thickness of the film could be mediated from 10 to several hundreds μm just by varying the fabrication conditions during the phase separation process. The surface and cross-sectional morphologies of CCH film are shown in Fig. 4**(d–f)**. One can see that CCH film showed a homogeneous, dense, and smooth surface without obvious separation of compositions indicating good compatibility between CCH and HCl. The cross-section was also compact and non-porous structure. This characteristic of the film would benefit for loading and maintaining of electrolyte ions via the free volume of flexible polymer chains, especially in swollen film [43].

The XRD patterns of pristine CCP and the crosslinked CCH film are shown in Fig. 4g. Pristine CCP exhibited semi-crystalline structure and had a distinct diffraction peak at the 2θ angle of 26.3° and a broad peak at about 20°, demonstrating that pristine CCP contained both crystalline and amorphous regions. After crosslinking, the peak at about 20° turned wider and its intensity became weaker. In addition, some of the weak peaks decreased or vanished. This was because the destruction of crystalline structure of carboxylated chitosan, or the reduction of crystallinity degree due to crosslinking. The characteristic of higher ratio of amorphous structure would be beneficial to obtaining high ionic conductivity for a gel polymer electrolyte. On the basis of Ratner and Shriver [44], the more flexible polymer chain, the better the ion mobility could be obtained, because that the ionic conductance of the gel polymer electrolyte occurs in amorphous phases. In this case, polymer chains would form a network structure through crosslinking, which inhibited the crystallization of the polymer so increased the absorption capacity of electrolyte in the polymer matrix, and finally improve the ionic conductivity.

The thermal decomposition of pristine CCP was divided into two stages. The first weight loss within 60–160 °C was attributed to the loss of moisture in the sample corresponding to the heat absorption peak of about 80 °C on the DSC curve. While the second stage weight loss in the

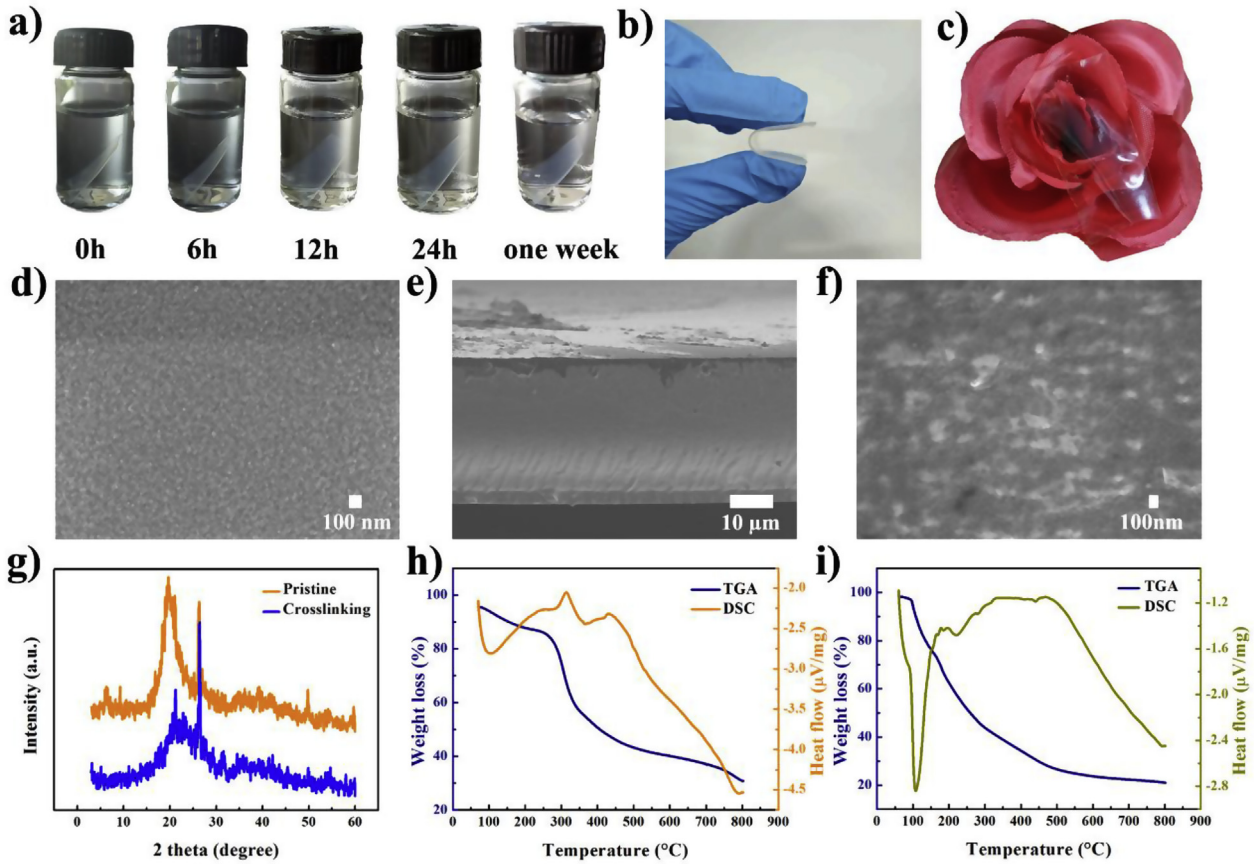

Fig. 4. a) Digital photos of CCH film immersed in water for different time, b) before and c) after freeze-drying, SEM images of the CCH film after freeze-drying: d) surface, e) cross-sectional, and f) high-magnification, g) XRD patterns, and TGA-DSC curves of h) pristine carboxylated chitosan powders and i) CCH film under N_2 atmosphere.

range of 250–500 °C was considered to the degradation of carboxylated chitosan skeleton. The temperature of exothermic peak corresponded to the degradation temperature of amino groups on the carboxylated chitosan chain (314 °C). Meanwhile, there was no glass transition temperature for carboxylated chitosan (Fig. 4h). Obviously, thermal stability of the CCH film decreased from the beginning without noticeable step, and two distinct endothermic peaks corresponded to the volatilization of water (107 °C) and the decomposition temperature of polymer chains (220 °C). It indicates that the thermal stability of the film was high, and it did not decompose within 100 °C. Besides, exothermic peak did not appear, indicating that the amino group was protonated, which is consistent with the previous results (Fig. 4i). The decomposition temperature of the CCH film decreased due to the fact that crosslinking process maybe destroy the crystallization of carboxylated chitosan, which is also consistent with the XRD results.

The ionic conductivity of the CCH film was calculated by the equation of $\sigma = L/(R_b A)$ according to Nyquist plot. As shown in Fig. 5a, the values of R_b, L, and A were 0.3622 Ω, 0.532 mm, and 1.69 cm^2, respectively, so the ionic conductivity was calculated to be 8.69×10^{-2} S cm^{-1}. In general, ionic conductivity of GPE was approximately 10^{-3} S cm^{-1} at ambient temperature. Interestingly, the ionic conductivity of the prepared CCH film in this work was much higher than the values reported in literature. Meanwhile, the electrolyte uptake rate of the film (W%) was also calculated by the equation of $W\% = M_{wet} - M_{dry}/M_{dry} \times 100\%$. The absorption rate of the CCH film attained 742%, higher than the other GPE films reported in the literature such as VSNPs-PAA [45], *C*S-MSA-15 [46], MPEs [47], mCel-membrane [7], and KCl-Fe^{3+}/PAA [36], as shown in Fig. 5b. The good electrolyte-absorption ability of CCH film attributed to the carboxylated chitosan chains containing a variety of hydrophilic groups and high compatibility with HCl electrolyte, which in turn benefited to improving the ionic conductivity.

The CCH film showed both high ions conductivity and high electrolyte uptake rate, so it could be used to fabricate the all-solid-state component and device for energy storage and conversions. In this work, all-solid-state EDLC was assembled and the electrochemical performance is shown in Fig. 6. Fig. 6a exhibits the schematic diagram of the assembled all-solid-state EDLC, which has three layers of components: activated carbon film, CCH film, and activated carbon film. Activated carbon film electrodes were prepared according to our previous report [37]. The carbon cloth was selected as the current collector, and the CCH film was sandwiched between the two symmetrical activated carbon electrodes. Giving some pressure to ensure the close contact between the current collectors, electrodes, and GPE during the testing process.

The electrochemical performance of all-solid-state EDLC was measured. The CV curves with a potential window of 0–0.9 V of EDLC at different scan rates showed quasi-rectangular shapes, indicating low charge transfer resistance and relatively ideal capacitance characteristics. As the scan rate increasing (up to 100 mV s^{-1}), the rectangular CV curve became leaf-like, showing that the charge transfer resistance became the dominant factor in the supercapacitor (Fig. 6b). The GCD curves measured within a potential window of 0–0.9 V at various current densities are displayed in Fig. 6c. As one can see, all the curves exhibited typical symmetric triangular shapes with a small internal resistance (IR) drop, further proving the ideal reversible capacitance characteristic of electric double layer capacitor. For the Nyquist plots (Fig. 6d), the plot consisted of a semicircle in the high frequency region and an inclined line in the low frequency region, showing its double layer capacitive behavior. The intercept in the high frequency region

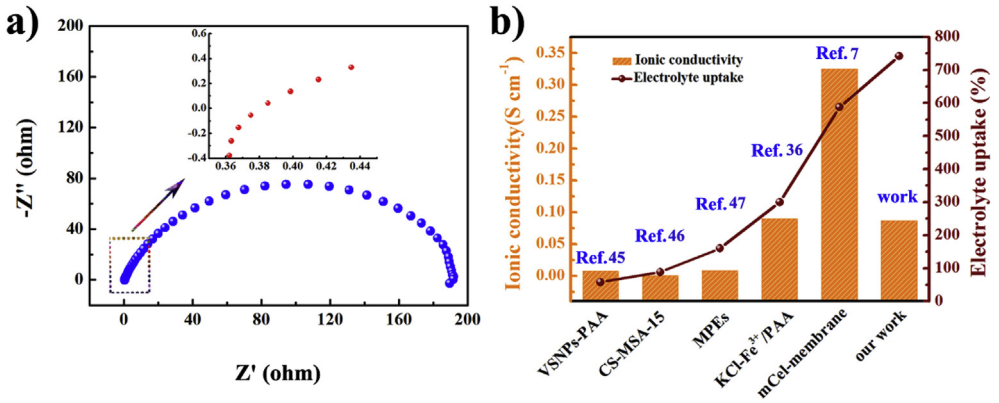

Fig. 5. a) Nyquist plot of the CCH film determined at room temperature, and b) the ionic conductivity and liquid electrolyte uptake rate of the CCH film compared with those from literature.

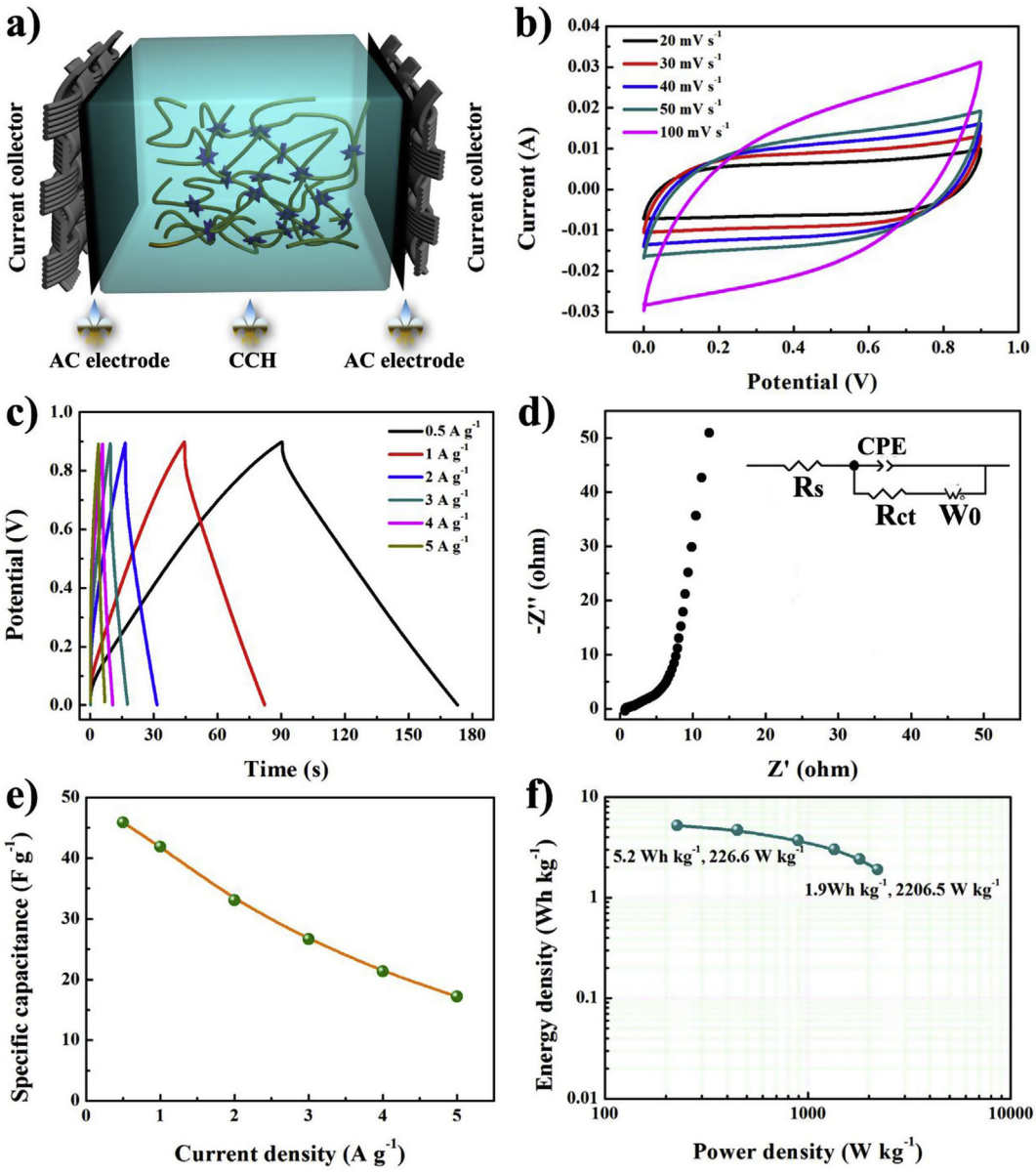

Fig. 6. a) Schematic diagram, and the electrochemical performance of the assembled EDLC device: b) CV curves at various scanning rates, c) GCD curves at various current densities, d) Nyquist plots, e) specific capacitances at different current density, and f) Ragone plot.

was the bulk resistance (R_s), which was influenced by the bulk resistance of GPE film and internal resistance of the electrode. The semicircle represented the charge transfer resistance (R_{ct}), which was associated with the electrode-electrolyte interface, bringing mainly about the ionic resistance. By fitting the equivalent circuit, the bulk resistance (R_s) was 1.229 Ω and the charge transfer resistance (R_{ct}) was 1.208 Ω, reflecting that the EDLC had low ion transport restriction at electrode-electrolyte interface and thus had a small interface resistance. In addition, it was proved that AC film electrode had a good compatibility with the CCH film. The linear region of slope was the Warburg impedance element (W_0) related to the ion diffusion resistance deriving from ions diffusion through porous electrodes. Moreover, the specific capacitances at different current densities are presented in Fig. 6e. The specific capacitances of device were 45.9, 41.9, 33.1, 26.7, 21.3, and 17.2 F g^{-1} measured at a current density from 0.5 to 5 A g^{-1}, respectively. They gradually decreased with the increase of current density, owing to a reduction in the diffusion of ions into the electric double layer electrode and the increase of electrical resistance of the material. Energy density and power density were important indexes for evaluating the electrochemical properties of supercapacitors. In Fig. 6f, the energy density of the device reached 5.2 Wh kg^{-1} at a power density of 226.6 W kg^{-1}, and remained 1.9 Wh kg^{-1} at a power density of 2206.5 W kg^{-1}.

4. Conclusions

In summary, we have successfully developed a novel GPE film by non-covalently crosslinking carboxylated chitosan polymer chains. The flexible and transparent CCH film possessed several advantages such as high flexibility, high electrolyte absorption capacity, and high ionic conductivity. Symmetric all-solid-state EDLC combining CCH film with activated carbon electrode exhibited high electrochemical performance. The maximum energy density of all-solid-state EDLC reached 5.2 Wh kg^{-1} at a power density of 226.6 W kg^{-1}, and a high power density of 2206.5 W kg^{-1} at 1.9 Wh kg^{-1} within 0–0.9 V potential window. Our research provides a promising and new direction for developing flexible energy storage devices in a rapid, easy, and low-cost way.

Acknowledgments

This work was partly supported by the National Natural Science Foundation of China (51203071, 51363014, 51463012, and 51763014), China Postdoctoral Science Foundation (2014M552509 and 2015T81064), Natural Science Funds of the Gansu Province (1506RJZA098), and the Program for Hongliu Distinguished Young Scholars in Lanzhou University of Technology.

References

[1] H. Sun, S. Xie, Y. Li, Y. Jiang, X. Sun, B. Wang, H. Peng, Large-area supercapacitor textiles with novel hierarchical conducting structures, Adv. Mater. 28 (38) (2016) 8431–8438.
[2] H. Li, C. Han, Y. Huang, Y. Huang, M. Zhu, Z. Pei, Q. Xue, Z. Wang, Z. Liu, Z. Tang, An extremely safe and wearable solid-state zinc ion battery based on a hierarchical structured polymer electrolyte, Energy Environ. Sci. 11 (4) (2018) 941–951.
[3] L. Kou, T. Huang, B. Zheng, Y. Han, X. Zhao, K. Gopalsamy, H. Sun, C. Gao, Coaxial wet-spun yarn supercapacitors for high-energy density and safe wearable electronics, Nat. Commun. 5 (5) (2014) 3754.
[4] Z. Pan, J. Yang, Q. Zhang, M. Liu, Y. Hu, Z. Kou, N. Liu, X. Yang, X. Ding, H. Chen, J. Li, K. Zhang, Y. Qiu, Q. Li, J. Wang, Y. Zhang, All-solid-state fiber supercapacitors with ultrahigh volumetric energy density and outstanding flexibility, Adv. Energy 9 (9) (2019) 1802753.
[5] Y. Yang, L. Zhao, K. Shen, Y. Liu, X. Zhao, Y. Wu, Y. Wang, F. Ran, Ultra-small vanadium nitride quantum dots embedded in porouscarbon as high performance electrode materials for capacitive energy storage, J. Power Sources 333 (2016) 61–71.
[6] L. Zang, Q. Liu, J. Qiu, C. Yang, C. Wei, C. Liu, L. Lao, Design and fabrication of an all-solid-state polymer supercapacitor with highly mechanical flexibility based on polypyrrole hydrogel, ACS Appl. Mater. Interfaces 9 (39) (2017) 33941–33947.
[7] D. Zhao, C. Chen, Q. Zhang, W. Chen, S. Liu, Q. Wang, Y. Liu, J. Li, H. Yu, High Performance, flexible, solid-state supercapacitors based on a renewable and biodegradable mesoporous cellulose membrane, Adv. Energy 7 (18) (2017) 1700739.
[8] D. Wu, W. Zhong, A new strategy for anchoring a functionalized graphene hydrogel in a carbon cloth network to support a lignosulfonate/polyaniline hydrogel as an integrated electrode for flexible high areal-capacitance supercapacitors, J. Mater. Chem. 7 (10) (2019) 5819–5830.
[9] W. Dong, Z. Wang, Q. Zhang, M. Ravi, M. Yu, Y. Tan, Y. Liu, L. Kong, L. Kang, F. Ran, Polymer/block copolymer blending system as the compatible precursor system for fabrication of mesoporous carbon nanofibers for supercapacitors, J. Power Sources 419 (2019) 137–147.
[10] C. Zhong, Y. Deng, W. Hu, J. Qiao, L. Zhang, J. Zhang, A review of electrolyte materials and compositions for electrochemical supercapacitors, Chem. Soc. Rev. 44 (21) (2015) 7484–7539.
[11] Y. Zhou, C. Wan, Y. Yang, H. Yang, S. Wang, Z. Dai, K. Ji, H. Jiang, X. Chen, Y. Long, Highly stretchable, elastic, and ionic conductive hydrogel for artificial soft electronics, Adv. Funct. Mater. 29 (1) (2019) 1806220.
[12] K. Wang, X. Zhang, C. Li, X. Sun, Q. Meng, Y. Ma, Z. Wei, Chemically crosslinked hydrogel film leads to integrated flexible supercapacitors with superior performance, Adv. Mater. 27 (45) (2015) 7451–7457.
[13] X. Peng, H. Liu, Q. Yin, J. Wu, P. Chen, G. Zhang, G. Liu, C. Wu, Y. Xie, A zwitterionic gel electrolyte for efficient solid-state supercapacitors, Nat. Commun. 7 (2016) 11782.
[14] Y. Huang, M. Zhong, F. Shi, X. Liu, Z. Tang, Y. Wang, Y. Huang, H. Hou, X. Xie, C. Zhi, An intrinsically stretchable and compressible supercapacitor containing a polyacrylamide hydrogel electrolyte, Angew. Chem. Int. Ed. 56 (31) (2017) 9141–9145.
[15] M. Yamagata, K. Soeda, S. Ikebe, S. Yamazaki, M. Ishikawa, Chitosan-based gel electrolyte containing an ionic liquid for high-performance nonaqueous supercapacitors, Electrochim. Acta 100 (2013) 275–280.
[16] L. Cao, M. Yang, D. Wu, F. Lyu, Z. Sun, X. Zhong, H. Pan, H. Liu, Z. Lu, Biopolymer-chitosan based supramolecular hydrogels as solid state electrolytes for electrochemical energy storage, Chem. Commun. 53 (10) (2017) 1615–1618.
[17] Y. Wan, K.A.M. Creber, B. Peppley, V.T. Bui, Ionic conductivity of chitosan membranes, Polymer 44 (4) (2003) 1057–1065.
[18] Y. Xiao, Y. Xiang, R. Xiu, S. Lu, Development of cesium phosphotungstate salt and chitosan composite membrane for direct methanol fuel cells, Carbohydr. Polym. 98 (1) (2013) 233–240.
[19] M.H. Buraidah, L.P. Teo, S.R. Majid, A.K. Arof, Ionic conductivity by correlated barrier hopping in NH4I doped chitosan solid electrolyte, Phys. B Condens. Matter 404 (8–11) (2009) 1373–1379.
[20] S. Fuentes, P.J. Retuert, G. González, Lithium ion conductivity of molecularly compatibilized chitosan-poly(aminopropyltriethoxysilane)-poly(ethylene oxide) nanocomposites, Electrochim. Acta 53 (4) (2008) 1417–1421.
[21] T. Winie, S.R. Majid, A.S.A. Khiar, A.K. Arof, Ionic conductivity of chitosan membranes and application for electrochemical devices, Polym. Adv. Technol. 17 (7–8) (2006) 523–527.
[22] Y. Wan, K.A.M. Creber, B. Peppley, V.T. Bui, Ionic Conductivity and tensile properties of hydroxyethyl and hydroxypropyl chitosan membranes, J. Polym. Sci. B Polym. Phys. 42 (8) (2010) 1379–1397.
[23] Y. Wan, K.A.M. Creber, B. Peppley, V.T. Bui, Chitosan-based electrolyte composite membranes: II. Mechanical properties and ionic conductivity, J. Membr. Sci. 284 (1) (2006) 331–338.
[24] J. Duan, X. Liang, Y. Cao, S. Wang, L. Zhang, High strength chitosan hydrogels with biocompatibility via new avenue based on constructing nanofibrous architecture, Macromolecules 48 (8) (2015) 2706–2714.
[25] N. Bhattarai, J. Gunn, M. Zhang, Chitosan-based hydrogels for controlled, localized drug delivery, Adv. Drug Deliv. Rev. 62 (1) (2010) 83–99.
[26] A. Primo, F. Quignard, Chitosan as efficient porous support for dispersion of highly active gold nanoparticles: design of hybrid catalyst for carbon-carbon bond formation, Chem. Commun. 46 (30) (2010) 5593–5595.
[27] S. Peng, H. Meng, Y. Ouyang, J. Chang, Nanoporous magnetic cellulose-chitosan composite microspheres: preparation, characterization, and application for Cu(II) adsorption, Ind. Eng. Chem. Res. 53 (6) (2014) 2106–2113.
[28] W. Wu, C. Xu, Z. Zheng, B. Lin, L. Fu, Strengthened, recyclable shape memory rubber films with a rigid filler nano-capillary network, J. Mater. Chem. 7 (12) (2019) 6901–6910.
[29] S.C. Chen, Y.C. Wu, F.L. Mi, Y.H. Lin, L.C. Yu, H.W. Sung, A novel pH-sensitive hydrogel composed of N,O -carboxymethyl chitosan and alginate cross-linked by genipin for protein drug delivery, J. Control. Release 96 (2) (2004) 285–300.
[30] C. Lingyun, T. Zhigang, D. Yumin, Synthesis and pH sensitivity of carboxymethyl chitosan-based polyampholyte hydrogels for protein carrier matrices, Biomaterials 25 (17) (2004) 3725–3732.
[31] X.G. Chen, Z. Wang, W.S. Liu, H.J. Park, The effect of carboxymethyl-chitosan on proliferation and collagen secretion of normal and keloid skin fibroblasts, Biomaterials 23 (23) (2002) 4609–4614.
[32] A. Anitha, V.V.D. Rani, R. Krishna, V. Sreeja, N. Selvamurugan, S.V. Nair, H. Tamura, R. Jayakumar, Synthesis, characterization, cytotoxicity and antibacterial studies of chitosan, O-carboxymethyl and N,O-carboxymethyl chitosan nanoparticles, Carbohydr. Polym. 78 (4) (2009) 672–677.
[33] J. Fu, M. in het Panhuis, Hydrogel properties and applications, J. Mater. Chem. B 7 (10) (2019) 1523–1525.
[34] Y.F. Huang, P.F. Wu, M.Q. Zhang, W.H. Ruan, E.P. Giannelis, Boron cross-linked graphene oxide/polyvinyl alcohol nanocomposite gel electrolyte for flexible solid-state electric double layer capacitor with high performance, Electrochim. Acta 132 (2014) 103–111.
[35] Q. Tang, M. Chen, G. Wang, H. Bao, P. Saha, A facile prestrain-stick-release

assembly of stretchable supercapacitors based on highly stretchable and sticky hydrogel electrolyte, J. Power Sources 284 (2015) 400–408.
[36] Y. Guo, X. Zhou, Q. Tang, H. Bao, G. Wang, P. Saha, A self-healable and easily recyclable supramolecular hydrogel electrolyte for flexible supercapacitors, J. Mater. Chem. 4 (22) (2016) 8769–8776.
[37] X. Zhao, F. Ran, K. Shen, Y. Yang, J. Wu, X. Niu, L. Kong, L. Kang, S. Chen, Facile fabrication of ultrathin hybrid membrane for highly flexible supercapacitors via in-situ phase separation of polyethersulfone, J. Power Sources 329 (2016) 104–114.
[38] S.P. Strand, S. Danielsen, B.E. Christensen, K.M. Varum, Influence of chitosan structure on the formation and stability of DNA-chitosan polyelectrolyte complexes, Biomacromolecules 6 (6) (2005) 3357–3366.
[39] C. Zheng, X. Yan, J. Si, Y. Meng, Z. Qi, Z. Tao, Ionic interactions between sulfuric acid and chitosan membranes, Carbohydr. Polym. 73 (1) (2008) 111–116.
[40] A.B. Lowe, C.L. Mccormick, Synthesis and solution properties of zwitterionic polymers, Chem. Rev. 102 (11) (2002) 4177–4189.
[41] A.B. Lowe, N.C. Billingham, S.P. Armes, Synthesis and characterization of zwitterionic block copolymers, Macromolecules 31 (18) (1998) 5991–5998.
[42] H. Walter, D. Forciniti, Cross-partitioning: determination of isoelectric point by partitioning, Methods Enzymol. 228 (1994) 223–233.
[43] K. Soontarapa, U. Intra, Chitosan-based fuel cell membranes, Chem. Eng. Commun. 193 (7) (2006) 855–868.
[44] M.A. Ratner, D.F. Shriver, Ion transport in solvent-free polymers, Chem. Rev. 88 (1) (1988) 109–124.
[45] Y. Huang, M. Zhong, Y. Huang, M. Zhu, Z. Pei, Z. Wang, Q. Xue, X. Xie, C. Zhi, A self-healable and highly stretchable supercapacitor based on a dual crosslinked polyelectrolyte, Nat. Commun. 6 (2015) 10310.
[46] V. Vijayalekshmi, D. Khastgir, Eco-friendly methanesulfonic acid and sodium salt of dodecylbenzene sulfonic acid doped cross-linked chitosan based green polymer electrolyte membranes for fuel cell applications, J. Membr. Sci. 523 (2017) 45–59.
[47] R. Na, G. Huo, S. Zhang, P. Huo, Y. Du, J. Luan, K. Zhu, G. Wang, A novel poly (ethylene glycol)–grafted poly(arylene ether ketone) blend micro-porous polymer electrolyte for solid-state electric double layer capacitors formed by incorporating a chitosan-based $LiClO_4$ gel electrolyte, J. Mater. Chem. 4 (46) (2016) 18116–18127.